JCSE The Journal of Corrosion Science and Engineering
ISSN 1466-8858 Volume 6, Preprint 111 submitted 10 August 2011

Study of Zn-Ni alloy coatings modified by nano-SiO_2 particles incorporation

*Olfa Hammami** [a,b], *Leila Dhouibi* [a], *Patrice Berçot* [b], *El Mustafa Rezrazi* [b], *Ezzeddine Triki* [a]

[a] Unit of Research « COPROMET » ENIT, BP 37, Belvedere, 1002 Tunisia.
[b] Institut UTINAM, CNRS UMR 6213, Équipe Sonochimie et Réactivité des Surfaces, Université de Franche-Comté, 16 route de Gray, 25030 Besançon Cedex, France.

Abstract

The aim of this research work was to co-deposit nano-SiO_2 particles into Zn-Ni alloy coatings in order to improve some surface properties. It had been investigated the effect of loading the plating bath with nanoparticles on composition, morphology, phase structure of deposits and their subsequent influence on the corrosion process in corrosive solution of 3% NaCl and the thermal stability of deposits at 200 °C. It was found that Zn-Ni alloy composites contain a higher percentage of Ni with incorporation in the deposit of 1.54 % of silica. X-ray diffraction measurements revealed that the alloys consisted of two phases, pure zinc and γ phase. Electrochemical characterization of the composites had been carried out through potentiodynamic polarization and electrochemical impedance spectroscopy. The composites exhibited higher values of microhardness and better corrosion resistance in corrosive media.

Keywords: Zn-Ni alloy; Composite coatings; Microhardness; Phase structure; GDOES; Corrosion

1. Introduction

The need for coatings with improved resistance to highly aggressive environments is high as a result of a growing demand for extended safe service life of industrial objects. Composite electrodeposition is a valuable new surface intensification technology to obtain composite coatings allowing to co-deposit inorganic and organic particles into the coatings in order to improve the surface properties. Several studies showed that electrochemically embedded particles impart special properties to composite coatings produced, which can meet the industrial request such as wear resistance, self-lubrication, corrosion resistance, etc...[1-3] Currently and for the foreseeable future, the most important types of nanoparticles are simple oxides, such as Al_2O_3, TiO_2 and SiO_2 used in established applications [4-6]. The particles of SiO_2 are hydrophilic and hence incorporate hardly into the surface of cathode. The main purpose of this research work was to co-deposit nano-SiO_2 particles into the Zn-Ni alloy coatings under direct current in order to improve the surface properties and the corrosion resistance in aggressive media.

* Corresponding author. Tel.: +21698909272
E-mail address: olfa.hammami@univ-fcomte.fr

JCSE The Journal of Corrosion Science and Engineering
ISSN 1466-8858 Volume 6, Preprint 111 submitted 10 August 2011

Then, the composite coatings had been characterized from compositional (EDX), morphological (SEM), structural (XRD) and depth profile (GDOES) points of view. In the meantime, electrochemical properties of the composite coatings had been studied by potentiodynamic polarization and electrochemical impedance spectroscopy.

2. Experimental

2.1. Electroplating process

The chemical compositions of the basic electrolytes of Zn–Ni alloys deposition are given in Table 1. All experiments were carried out in duplicated and the ability to reproduce of these measurements was found satisfactory.

Table 1: Solutions composition and conditions for alloy plating

Electrolyte ingredients	*Concentration* ($g.L^{-1}$)	*Plating parameters*
$ZnSO_4 . 7H_2O$	57.5	pH = 2,5 Temperature (°C) : 30 ± 0.5
$NiSO_4 . 6H_2O$	52.5	
H_3BO_3	9.3	
Na_2SO_4	56.8	
H_2SO_4	0.53	

Galvanostatic measurements were performed on steel rod cathode which was placed in a PTFE mount for obtaining cross-sectional area of 0.2 cm^2 in contact with solution. The deposition was done on steel (STUB 100CR6) substrates. The chemical composition of STUB 100CR6 steel was 0.95% C, 0.2%, Mn 0.15% Si and 0.015% S (wt %). Initially, the steel samples were mechanically polished with successively finer grades of emery paper. They were then washed in de-ionized water. This procedure was repeated until a clear and smooth surface was obtained. To obtain fixed hydrodynamic conditions, the Zn-Ni coatings were deposited on a rotating disc electrode (RDE) with a constant rotation velocity of 1000 rpm. The deposition experiments were performed at a current density of 25 mA/cm^2 and the plating time was 15 min. The SiO_2 powder (AEROSIL 200) with a mean diameter of 12 nm was used as received without any pre-treatment.
Before electrodeposition, the nanoparticles were dispersed in the bath by ultrasonic wave for 30 min. Particles with concentration of 5 g/L were maintained in an electrolytic bath in suspension by continuous magnetic stirring of 200 rpm for at least 24 hours before deposition.

2.2. Electrochemical measurements

For potentiodynamic measurements the coated samples were exposed to 3 % NaCl solution. These studies were performed respectively with potentiostat PGP 201 and interface Solarton SI 1287 /SI 1250 in a thermostatic three-electrode cell. The working electrode was a coated sample, the counter electrode was platinum with an

ISSN 1466-8858 Volume 6, Preprint 111 submitted 10 August 2011

area of 1 cm^2 and the reference electrode was saturated calomel SCE (Hg/Hg_2Cl_2/ KCl satured). The deposition and potentiodynamic stripping processes were performed in a non-agitated electrolyte.

2.3. Characterization studies

An X-ray diffraction investigation of Zn-Ni electrodeposits was carried out using an X-ray diffractometer D8 (Advance Bruker) equipped with a copper anode generating Ni-filtered CuKα radiation (l = 1.5405 A°, 45 KV, 40 mA). The quantity of Zn and Ni in the coatings and their thicknesses was determined by the means of Fiscerscope X-Ray XDAL fluorescence. Surface morphology of the deposits was followed with electron microscope at 15 KV. Measurements of the Vickers microhardness (HV) of deposits were performed in the surface by using a HMV-M3 SHIMADZU Microhardness tester under 25 g to 100 g load for 10 s and the corresponding final values were determined as the average of 5 measurements.

Glow discharge optical emission spectroscopy (GDOES); the distribution of species in the deposit was determined by depth profiling using a Jobin Yvon GD Profiler instrument equipped with a 4 mm diameter anode and operating after optimization at a pressure of 650 Pa and a power of 30 W in an argon atmosphere. This low power was retained to decrease the speed of abrasion of the deposits with low thickness and to obtain maximum information at the surface. Quantified compositional results were evaluated automatically utilizing the standard Jobin Yvon quantum Intelligent Quantification software. The instrument was calibrated with standard with known composition. Depths were calculated using relative sputter rates, obtained from the sputter yields of each major element with corrections for composition and discharge conditions.

3. RESULTS AND DISCUSSION

3.1 Behavior of SiO_2 nanoparticles in the plating solution

In table 2, we regrouped zeta potential and electrophoretic mobility measurements of particles suspended in the electroplated solution diluted 100 times. By observing the movement of particles under the influence of an electric field in the airframe microelectrophoresis "Rank Brothers II", we can determine the effective charge of particles and calculate the electrophoretic mobility of the particle and its corresponding zeta potential.

Table 2: Electrophoretic mobility and Zeta potential measurements by « Rank Brother II »

pH of bath solution	Effective charge of SiO_2 particles	Electrophoretic mobility ($cm^2.V^{-1}.s^{-1}$)	Zeta potential (mV)
6.7	-	$1.45\ 10^{-8}$	18.6

We noted negatively charged particles of SiO_2. This type of oxide is hydrophilic, so it always interacts with the electrolyte and therefore chemical and physical adsorption

ISSN 1466-8858 Volume 6, Preprint 111 submitted 10 August 2011

of electrolyte ions onto the particle occurs. This adsorption and the initial particle surface composition determine the particle surface charge, which induces a double layer of electrolyte ions around the particle. In electrolytes, double layers play a major role in the interactions between particles and also between particles and the electrode [7]. In aqueous media, due to protonation / deprotonation of the superficial groups can change also the surface charge of the oxide particles depending on the solution pH [8]. The absolute value of the zeta potential is a very important factor for the degree of particles incorporation. In fact, zeta potential determined the static electricity force among nano-SiO_2 particles and influenced greatly the character either agglomeration or dispersion among the nano-particles [9]. When the nano-particles of SiO_2 became close to the cathode, the repulsion force among the double charge layers of nano-particles increased, the possibility of conglobation among nano-particles decreased. In addition, the positive / negative of the zeta potential on the nano-particle surfaces had the crucial influence to the interaction among nano-particles and cathode surface during electrodeposition. So the stability of the composite electrodeposition solution could be characterized by the zeta potential on the nano-particle surfaces.

It can be seen from table 2 that, in pH 6.7, the value of zeta potential was low, showing that in the composite electrodeposition solution, nano-SiO_2 particles were easily adsorbed by the negative ions from sulphate radical, the conglobation trend among nano-particles weakened and the dispersibility of the composite electrodeposition solution was improved[9].

3.2 Compositional analysis, morphology and depth profile of Zn-Ni alloy coatings

The ratio of the less noble metal (Zn) to the more noble metal (Ni) in the deposit is larger than in the bath. This phenornenon is known as "anomalous codeposition", fully described by Brenner [10]. We obtained this type of Zn-Ni alloy deposits with a Ni content of 6.3 % (table 3). In comparison, X-ray fluorescence analysis of the coatings elaborated in the presence of SiO_2 nanoparticles showed about a double percentage of Ni in the deposit.

Table 3: Composition Analysis of Zn-Ni deposits by X-Ray fluorescence

Coating systems	Ni (± 0.2 wt. %)	Zn (± 0.2 wt. %)
Zn-Ni	6.3	93.7
Zn-Ni /nano-SiO_2	12.3	87.7

The surface morphology of Zn-Ni alloy coating had shown branched acicular crystallite structure (Fig.1-a). The surface of the composite coating (fig.1-b) seems to keep the same appearance with piled and smooth grains. EDS analysis of the composite coating surface revealed a silica content of 1.54 %.

JCSE The Journal of Corrosion Science and Engineering
ISSN 1466-8858 submitted 10 August 2011

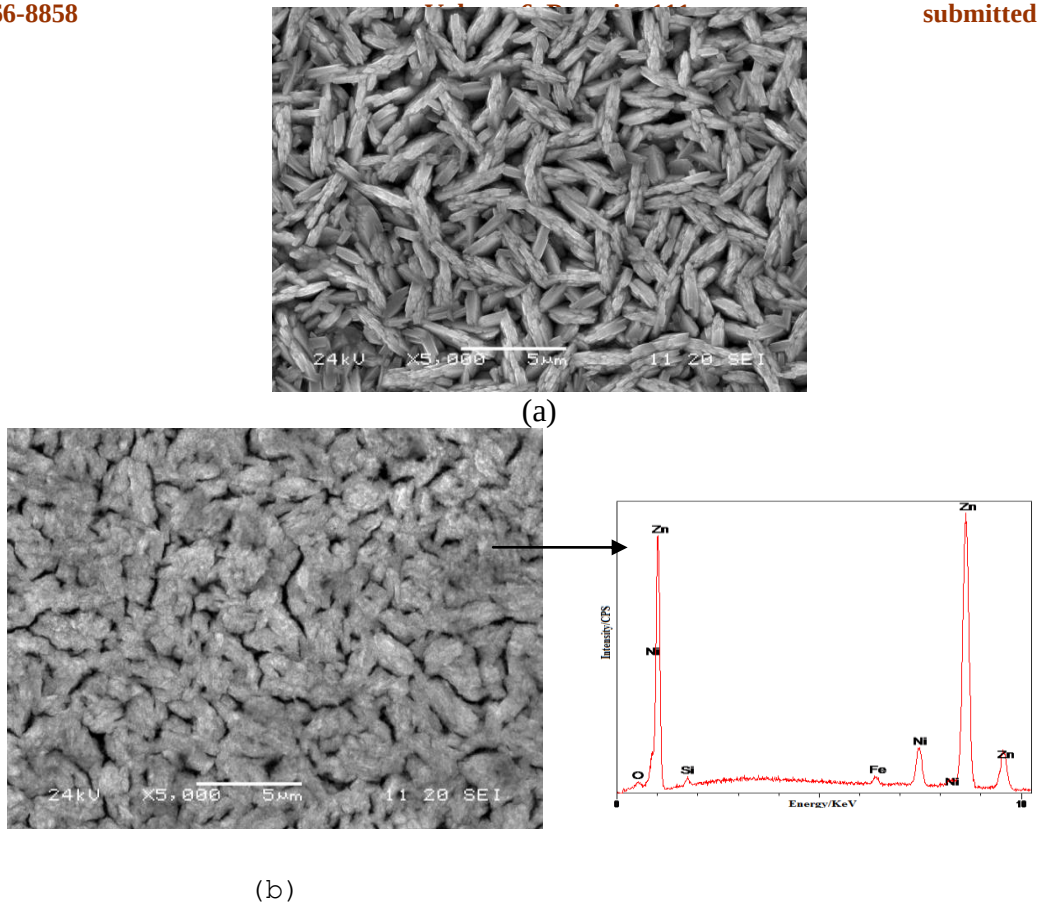

Figure 1 *: SEM micrographs and EDS of the surfaces of Zn-Ni-coated steel in plating bath : (a) Zn-Ni without nanoparticles, (b) Zn-Ni/5 g/L SiO_2*

Fig.2 showed the GDOES depth profile of the wt.% amount of the selected elements: zinc, nickel, silicium and iron for the Zn-Ni composite coating. The distributions of the different species are revealed clearly with sharply defined interface between the deposit and the substrate. The thickness of the composite measured by GDOES correlate very well with the one obtained by X-ray fluorescence (approximately 7 µm). Zinc and nickel species are incorporated relatively uniformly along the cross-section as depicted in Fig.2. Just in the outer region of the film, we confirm the presence of silicium which decreased until a depth of approximately 0.5 µm.

JCSE The Journal of Corrosion Science and Engineering
ISSN 1466-8858 tted 10 August 2011

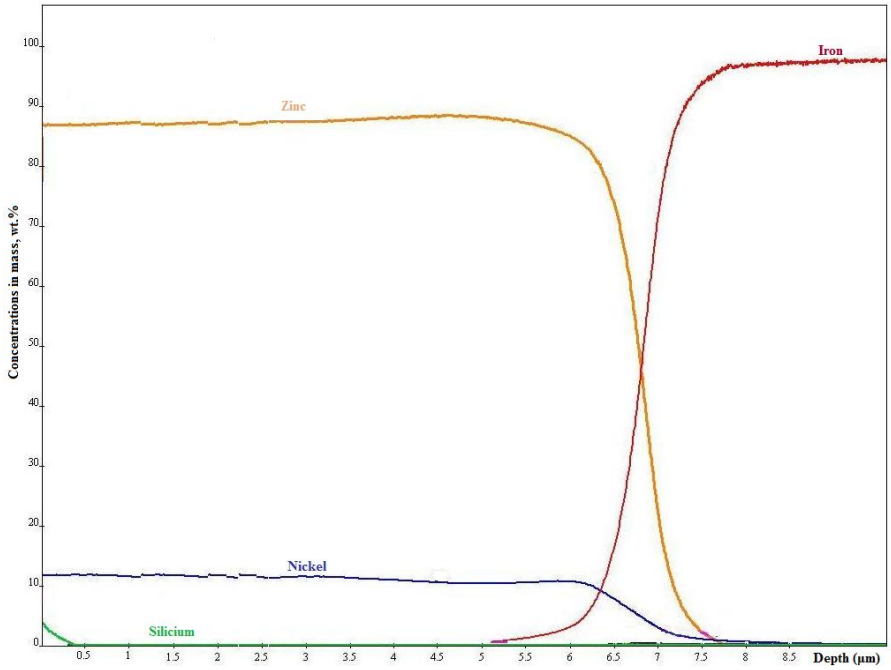

***Figure 2**: GDOES depth quantified profile of the Zn-Ni composite coating electrodeposited with (*25 mA/cm^2, 15 min) onto steel substrate.

3.3 Phase structure and microhardness

Fig.3 showed the XRD patterns for the plated Zn-Ni alloy coatings. It is clear that no significant change of phases content in spectra resulted from loading the plating bath with nano-SiO_2 particles. Only the diffraction lines of zinc and γ-phase of Zn-Ni alloys were observed. However, the peak of Fe (211) in the composite diffractogram disappeared giving rise to a deposit covering the surface of steel better than Zn-Ni alloy coating.

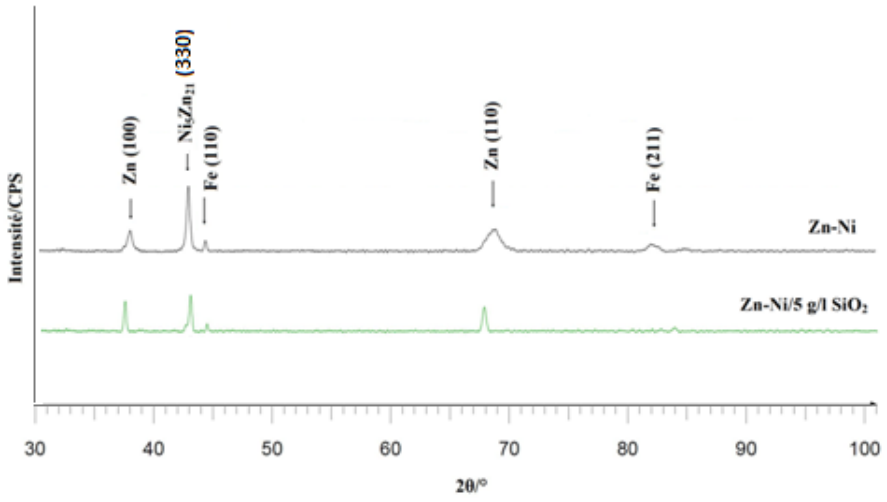

***Figure 3 :** X-ray diffractograms for the coatings* Zn-Ni electroplated without/and with nano-SiO_2 particles

JCSE The Journal of Corrosion Science and Engineering
ISSN 1466-8858 Volume 6, Preprint 111 submitted 10 August 2011

Crystallite sizes of the coatings were calculated from the X-ray peak broadening of the (330) diffraction peak using Scherrer's formula [11];

$$D = K\lambda/(\beta \cos\theta)$$

where, K is the Scherrer factor ≈1, D is the crystallite size, λ is the incident radiation wavelength, β is the integral breadth of the structurally broadened profile and θ is the angular position.

Zn-Ni alloy deposit exhibited a crystallite size of 50 nm, whereas the crystallite size of Zn-Ni composite coating decreased to 26 nm. We could explain this evolution by the fact that the nanoparticles of silica might perturb the crystal growth by increasing the number of nucleation sites and consequently a reduction in the grain size occurs as reported by Pavlatou and al [1]. Namely, the growth of the electrodeposited layer is a competition between the nucleation and crystal growth. Nanoparticles provide more nucleation sites and hence retard the crystal growth; subsequently the corresponding Zn-Ni matrix in the composite coating has a smaller crystal size. Moreover, the Ni content of Zn-Ni alloy coatings plays a major role in controlling the phases present and the grain size [12].

Vickers microhardness (HV) values of pure Zn-Ni coating and composite Zn-Ni/nano-SiO_2 deposits are shown in Fig.4.

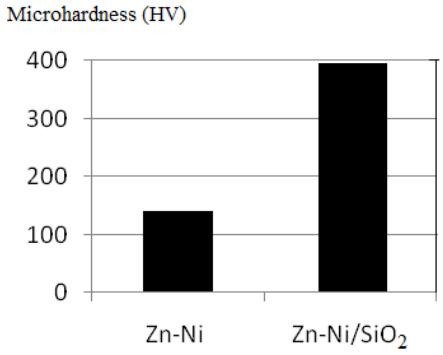

Figure 4 *: Evolution of microhardness of Zn-Ni alloy coatings*

The evolution of coatings hardness showed an increase from about 140 HV for pure Zn-Ni alloy to about 396 HV for samples prepared with SiO_2 particles. We can conclude that the microhardness was affected by the incorporation of this type of nanoparticles into deposits. The grain size, in turn, is an important variable affecting the hardness value usually expressed by Hall-Petch relation;

$$H = H_o + k/(d)^{1/2} \text{ [13]}$$

where H is microhardness of the material, d is crystallite size, H_o and k are experimental constants and are different for each material.

ISSN 1466-8858 Volume 6, Preprint 111 submitted 10 August 2011

Smaller crystallite size implies a greater number of grain boundaries that impede dislocation motion, and then creates harder materials.

3.4 Thermal stability

The thermal stability of Zn-Ni alloy electrodeposits is important to their general evaluation for future applications, particularly in applications where the coatings are expected to perform at elevated temperature such as on some automotive parts. In this study, we used the evolution of microhardness (fig.5) to evaluate the stability of coatings. Although a little decrease of composite deposits hardness values after 30 min of exposure to a temperature of 200 °C, the thermal stability studies showed that these deposits were thermally stable up 24 h and maintained higher values of microhardness than Zn-Ni alloy coatings.

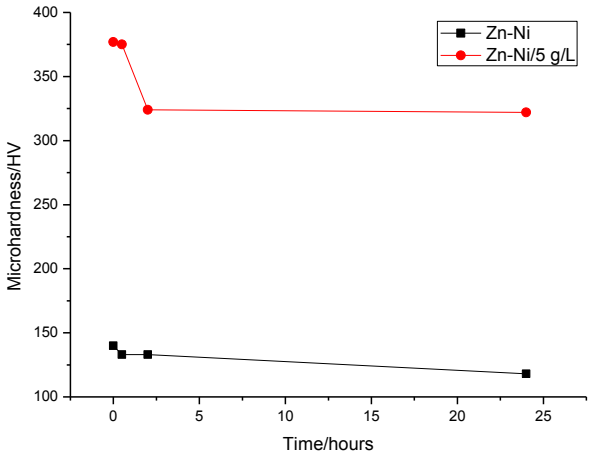

Figure 5 *: Variation of microhardness of* Zn-Ni alloy deposit and coating composite after heat treatment at 200 °C for 30 min, 2h and 24h.

3.5 Corrosion behavior of Zn-Ni/nanoparticles in 3% NaCl solution

3-5-1 Potentiodynamic polarization studies

During the anodic scan (Fig.6), distinct peaks were observed which could be attributed to the dissolution of Zn-Ni alloy components [14, 15] in the corroding media of 3% NaCl. Based on X-ray diffractograms of fig.3 and the potentials at which these peaks occur, we could make a qualitative estimate of Zn-Ni alloy composition. The first peak that is seen at around -800 mV/SCE corresponds to the Zn dissolution in η-phase. The potential, at which the peak occurred -600 mV/SCE, can be thought to be due to the dissolution of γ-phase, whereas the third dissolution peak is attributed to the dissolution of α-phase.

JCSE The Journal of Corrosion Science and Engineering
ISSN 1466-8858 Volume 6, Preprint 111 submitted 10 August 2011

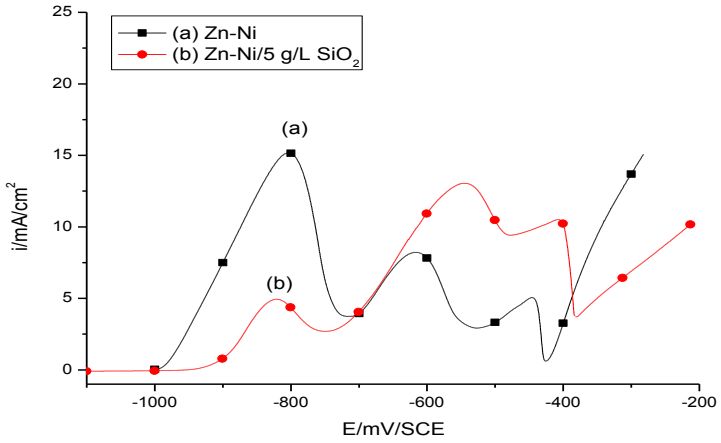

Figure 6 *: Anodic polarization curves of the substrates of steel coated with Zn-Ni alloy without/in the presence of 5 g/L SiO_2 under DC ; immersion : 3% NaCl, v = 25mV/min*

Fig.6 showed a decrease of the intensity of the first peak when we added nanoparticles in the plating bath. It suggests a reduce of the electrochemical kinetics of Zn-Ni composite. We calculated, from table 4, their rate of dezincification (2%) in comparison to the dezincification rate of Zn-Ni alloy coating (24%). In fact, dissolution of η-phase would expose the nickel-rich phase to the environment. A small defect in the coating in such a case would lead to the preferential dissolution of the less noble metal, namely, steel. Thus, an increase in life of the protective coating would simply depend on the life of the more electronegative phase, which is a Zn-rich η phase. Also, there was a clear shift for second and third peaks toward the noble direction, giving rise to an increase in corrosion resistance and of Zn-Ni composite coating. Furthermore, composites with higher Ni content (table 3) tend to dissolve slower than those with lower Ni content. This behavior indicates that Ni content by itself and the morphologies formed on the surface associated with it, are responsible for the observed corrosion behavior of the coatings.

3-5-2 Electrochemical impedance spectroscopy

EIS was used to evaluate the barrier properties of the coatings and to determine their polarization resistance. Fig.7 presented a comparison of Nyquist responses obtained for Zn-Ni elaborated without/ and with nano-SiO_2 particles under the same quantities of electricity. Two semicircles are generally observed in the complex-plane representation of the EIS data.

JCSE The Journal of Corrosion Science and Engineering
ISSN 1466-8858 Volume 6, Preprint 111 submitted 10 August 2011

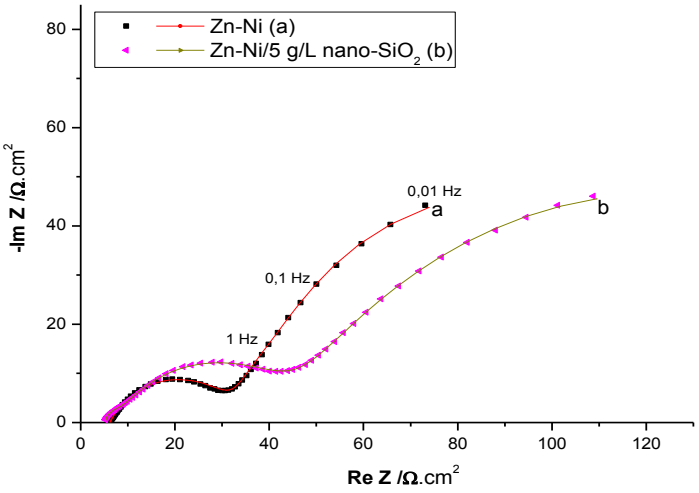

Figure 7 *:* Complex plane plots obtained for Zn-Ni alloy coating and Zn-Ni composite coating, after immersion in 3% NaCl solution during 24 h.
Symbols are the experimental data and lines were modeled using fitting model

The Nyquist-like diagram of the samples is characteristic of electrode process under kinetic and charge transfer control. R_p values could be approximately determined by fitting the Nyquist response to a simple equivalent circuit consisting of the solution resistance, a time constant in the high frequency represented by (C_f x R_f) attributed to film surface, double layer capacitance, and polarization resistance. R_f was very small and cannot be clearly separated from the kinetic part of the Nyquist representation. In all cases, the proposed model was in total agreement with the experimental data. The polarization resistance of Zn-Ni alloy coatings, determined by fitting with the model and summarized in the table 4, was improved with loading nano-SiO_2 particles in the plating bath. In addition, the corrosion potential shifted to positive values (table 4) indicating a change in the content ratio in the alloy and higher corrosion resistance compared with the Zn-Ni alloy coating.

Table 4: E_{corr} and R_p of Zn-Ni alloy deposits immersed in 3% NaCl solution for 24 h

Deposits	Composition analyses (± 0.2 wt. %)				Open-circuit potential (E_{corr} mV/SCE)	Polarization resistance (R_p Ω)
Zn-Ni	Zn	Ni	Cl	Fe	-1020	320
	71	6	10.8	1.3		
Zn-Ni /nano-SiO_2	85.8	9.73	4	0.47	-941	560

We could observe from fig.8-a an alternation of zones presenting defects (micro cracks), and zones more uniform with grains of salt in clusters deposited on the coating. The better electrochemical performance of the composite coating may be

ISSN 1466-8858 Volume 6, Preprint 111 submitted 10 August 2011

attributed to the reduction in the defect size by the incorporation of nanoparticules, which may be also helpful to segregate the corrosion products (appeared in a thin layer) as we could see from figure 8-b. In fact, in comparison with Zn-Ni alloy coating, the percentage of Fe and Cl in the composite decreased (table 4).

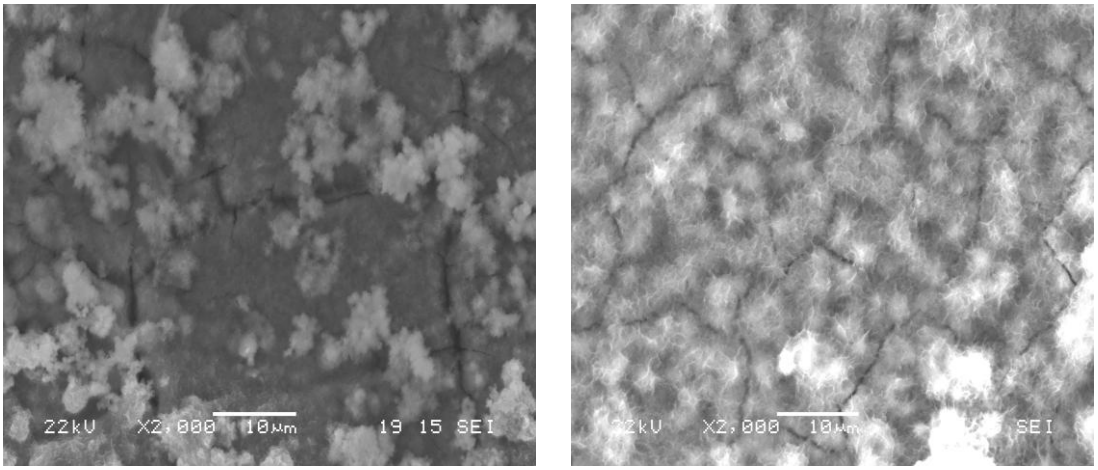

(a) (b)

Figure 8 *: Comparison of SEM micrographs of the surfaces of Zn-Ni alloy coatings* after immersion in 3% NaCl solution during 24 h *: (a) Zn-Ni electroplated without nanoparticles, (b) Zn-Ni/5 g/l* SiO_2

4. Conclusion

This work represented the electrodeposition and corrosion of Zn-Ni composite coating elaborated in the presence of SiO_2 nanoparticles in the plating bath in comparison with Zn-Ni alloy coating. This study was made to evaluate the influence of nanoparticles addition on some properties such as hardness, morphologic and structure characteristics. In comparison with Zn-Ni alloy coatings, the results revealed that Zn-Ni alloy composites

- revealed a higher percentage of Ni and an incorporation of 1.54 % of silica in the deposit.
- formed a mixture of two phases ; pure zinc and γ phases, with smaller cristallite size.
- exhibited higher values of microhardness and were thermally stable up 24 h at 200 °C.
- revealed better corrosion resistance in corrosive media of 3% NaCl solution.

Acknowledgements

The authors would like to acknowledge the financial support provided by “Action Intégrée Franco-Tunisienne du Ministère des Affaires Etrangères et Européennes français et du Minstère de l’Enseignement Supérieur, de la Recherche Scientifique et de la Technologie tunisien”.

References

ISSN 1466-8858 Volume 6, Preprint 111 submitted 10 August 2011

[1] E.A. Pavlatou, M. Stroumbouli, P. Gyftou, N. Spyrellis, J. Applied Electrochemistry, **36** (2006) 385-394.
[2] P. Gyftou, M. Stroumbouli, E.A. Pavlatou, P. Asimidis, N. Spyrellis, J. Electrochemica Acta, **50** (2005) 4544.
[3] N.K. Schrestha, D. B Hamal, T. Saji, J. Surface and Coatings Technology, **183** (2004) 247-253.
[4] S. Kim, J.J. Gislason, and al., J. Materials Chemistry, **16** (2004) 2336-2343.
[5] P.A. Janeway, American Ceramic Society Bulletin, **82** (2003) 31-38.
[6] B. Losiewicz, A. Stepien, D. Gierlotka, A. Bundiok, J.Thin Solid Films, **349 (**1999) 43.
[7] A.J. Hovestad, L.J.J. Janssen , Modern Aspects of Electrochemistry, Ed. by B. E. Conway, **38** (2004) 543.
[8] H.P.G. Simunkova, P. Wosik, J. Angerer, P. Kronberger, G.E. Nauer, J. Surface and Coatings Technology, **203** (2009) 1806-181.
[9] P.C. Hiemenz, Principles of Colloid and Surface Chemistry, Ed. by Marcel Dekker **2** (1986) 815.
[10] Brenner A., Electrodeposition of alloys, Principles and Practice, Ed. by I&EC Analytical **2** (1963) 194.
[11] H.P. Klug, L.E. Alexander, X-Ray Diffraction Procedures, Ed. Chapman and Hall, **7** (1959) 681.
[12] A. Alfantazi, A.M. El-Sherik, U. Erb, J. Scripta Metallurgica et Materialia, **30** (1994) 1245-1250.
[13] A. Portinha, V. Teixeire, and al., J. Surface and Coatings Technology, **200** (2005) 765.
[14] S.K. Zecevic, J.B. Zotovic, S.L. Gojcovic, V. Radmilovic, J. Electroanalytical Chemistry, **448** (1998) 245.
[15] S. Swathirajan, J. Electrochemical Society, **221** (1987) 211.